Characterization of interfacial water at hydrophilic and hydrophobic surfaces by in situ **FTIR**/internal reflection spectroscopy

M.R. Yalamanchili, A.A. Atia, J. Drelich and J.D. Miller
412 William C. Browning Building,
Department of Metallurgical Engineering,
College of Mines and Earth Sciences,
University of Utah,
Salt Lake City, Utah 84112, U.S.A.

ABSTRACT

In-situ FTIR/internal reflection spectroscopy (FTIR/IRS) has been used to spectroscopically characterize interfacial water near hydrophilic (silicon single crystal) and hydrophobic (polymer-coated germanium single crystal) surfaces. Interfacial water was examined spectroscopically over certain distances from the surface by appropriate design of the geometry and optics of the internal reflection system. The in-situ FTIR/IRS spectra were characterized by consideration of the OH stretching region (3000-3800 cm^{-1}) associated with the vibrational spectra of the interfacial water. Preliminary spectral results indicate the prevalence of an ice-like structure at the hydrophilic silicon surface, whereas at the hydrophobic surface the ice like structure is not so prevalent and there appears to be a significant decrease in hydrogen bonding.

INTRODUCTION

The characterization of interfacial water structure near hydrophilic and hydrophobic surfaces is of great importance in colloid and surface science areas including flotation, solid-liquid separation, dispersions and emulsions, flocculation, adsorption, and corrosion as well as in the preparation of thin films (1-4). Recent research suggests that the structural features of interfacial water determine the nature of interaction forces which control the aforementioned phenomena (5). Thus it is expected that the fundamental aspects of wetting phenomena are determined to a great extent by the structure and properties of interfacial water. For example, the nature and behavior of thin films during bubble attachment at the surface of a hydrophobic particle and the stability of water films in the froth phase are excellent examples of the importance of interfacial water in the flotation process. It has become evident then that the characterization of interfacial water is very important in understanding the so called non-DLVO interparticle forces (structuraVhydration forces) and their influence on particle dispersion and aggregation in aqueous systems. Several researchers (5) have provided experimental evidence for the existence of these short-range forces. Specifically, the attractive forces measured between hydrophobic surfaces were found to have decay lengths up to about 50 nm (6). However, the origin of these forces is still unknown although it is **M**'itfcly believed *that* changes in ihe interfacial water structure are responsible for the existence of such hydrophobic attractive forces (7,8).

Although there has been some progress in the area of modeling the structure of water near surfaces, there is very little experimental evidence to support the model predictions. In part, this has been due to the lack of a suitable technique to examine interfacial water structure. However, in recent years new analytical techniques have been developed such as internal reflection spectroscopy (IRS) and nonlinear optical spectroscopy, to study solid/liquid interfaces (9-11). Already, these techniques have opened up new avenues to probe solid/liquid interfaces in-situ with much improved surface sensitivities. Each of these spectroscopic techniques has its advantages and disadvantages with respect to the characterization of interfacial water.

The non-linear optical spectroscopy techniques such as second harmonic generation (SHG) and sum frequency generation (SFG) which are based on second-order non-linear optical processes occurring at solid/liquid interfaces provide for extremely high surface sensitivities and thus the characteristics of monomolecular interfacial species can be studied (10,11). However, these techniques can not be used to simultaneously detect both surface and bulk species since these non-linear processes are forbidden in centrosymmetric media such as bulk water. On the other hand, internal reflection spectroscopy (IRS) with reactive internal reflection elements can provide spectral information regarding both surface and bulk species. The use of IRS in conjunction with mid-FTIR, near-FTIR, and Raman spectroscopy techniques will allow for a systematic depth profiling of water from the surface *into* the *bulk. The* drawback of this technique is the relatively low surface sensitivity which prevents the isolated examination of the first few layers of water although a region as small as 30 nm from the surface can be examined (12). Since most of the signal (absorption) comes from the first few layers at the surface, as will be evident from discussion in the following sections, in-situ IRS can provide important information about interfacial water properties.

SPECTRAL FEATURES OF WATER STRUCTURE

There is considerable spectroscopic evidence which supports the existence of structure in liquid water. However, the interpretation of this evidence is varied and numerous models have been advanced in the past to explain the experimental results. These models generally fall into one of two broad categories viz. mixture and continuum models (13,14). Briefly, mixture models of liquid water assume the existence of two types of water molecules: hydrogen bonded and non-hydrogen bonded. The unbonded water molecules are identified as monomelic water and the bonded water may have many different species depending on the number and configuration of the hydrogen bonds. On the other hand, continuum models assume that all water molecules are tetrahedrally coordinated as in ice and there is very little, if any, hydrogen-bond breakage. These continuum predict that the distorted hydrogen bonds give rise to a continuous distribution of hydrogen bond strengths resulting in a broad OH stretching spectrum.

Each of the above approaches explains certain properties of water but leaves other characteristics unexplained. For example, the observation of a band near 3600 cm^{-1} which has been attributed to broken

hydrogen bonding (free OH) is not accounted for by the continuum models. It is not the intention of the authors of the present work to consider these opposing theories in greater detail. An excellent treatment of these two approaches to explain the structure of liquid water is given elsewhere (13). In the following paragraph, the general spectral characteristics that reveal the structure of water are considered.

Three different bands centered about 3600, 3400, and 3200 cm' have been identified in the OH stretching region of the vibrational spectra for water as shown in Table 1. The *OH* stretching bands were observed to shift from above 3600 cm"' at high temperature to below 3200 cm' in the spectra of ice at low temperature. Spectral features between 3000 and 3500 cm"' are generally attributed to the existence of hydrogen bonded OH stretching with different degrees of bond ordering. For example, the peak at - 3600 cm"' is attributed to the non-hydrogen bonded free OH stretching vibration. The peak at - 3400 cm"' has been assigned to a water structure with partial hydrogen bonding and the peak at - 3200 cm"' is generally attributed to the symmetric OH stretching mode associated with tetrahedrally coordinated water molecules as in ice. In any event, these spectral features in the OH stretching region can be used as indicators of the degree of hydrogen bonding, in other words, the degree of structure present in water.

Table 1. Spectral features of water structure in the OH stretching region

Region	Band Position (cnr')	Band Assignment	Kef.
3600 cm' Free Water or Weak Hydrogen Bonding	3715	Free OH Stretch	15
	3691	Free OH Stretch	16
	3682	Free OH Stretch	17
	3680	Free OH stretch	IS
	3650	Free OH Stretch, High Temp.	17
	3620-3650	Free OH Stretch	19
	3615	Free OH Stretch	20
3400 cm"' Incomplete Tetrahedral Coordination or Hydrogen Bond Disorder	3446 and 3496	Sym and Ami Sym OH Stretch	21
	3450	Bonded OH Stretch	21
	3420	Bonded OH Stretch Bifurcated hydrogen bonds	20
	3400	Bonded OH Stretch One H strongly bonded and the other weakly bonded	17
	3400	Bonded OH Stretch in H-bonded clusters	22
	3380	Bonded OH Stretch H-Bonding between oxygens	23
3200 cm' Complete Tetrahedral Coordination	3200	OH Stretch Ice-like Structure	17
	3200	Coupled Sym OH Stretch Tetrahedrally coordinated water	18
	3200	OH Stretch, Supercooled ice	24
	3200	OH Stretch, Ice-like structure	12

RESEARCH OBJECTIVES

In this present work, the in-situ FTIR internal reflection spectroscopy (IRS) technique was used to study in real time the structure of the interfacial water present at various depths from the surface under consideration. Silicon/water and polyraer-coa led germanium/water systems were selected as model systems to study the spectral characteristics of interfacial water as a function of distance from the surface by in-situ *FUR/IRS in* the MIR region. The spectral features including band position, shape, and intensity were examined at different distances from the surface in order to distinguish surface water from bulk water. Specifically, the OH stretching region of the vibrational spectra for interfacial water was studied in order to examine the degree of water structuring as a function of distance from the interface and as a function of temperature.

FTIR/IINTERNAL REFLECTION SPECTROSCOPY

Total Internal Reflection

Internal reflection spectroscopy (IRS), alternatively referred to as attenuated total reflection <ATR) spectroscopy, allows for in-situ real time spectroscopic measurements of interfacial phenomena. Consequently, IRS has become a powerful analytical tool for in-situ surface analysis in many areas of colloid and surface science (25). Shown in Figure 1 is a schematic representation of a ray of light undergoing total internal reflection in a parallelpiped shaped internal reflection element (IRE). Two requirements must be met before total internal reflection can occur. First, the IRE must be optically denser, that **is,** have a higher refractive index, than the sample ($n > n_2$). Second, the incident angle of the light beam in the IRE must be greater than a critical angle, θ_c:

$$\theta_c = \sin^{-1}(n^{\wedge}) \quad (1)$$

where n_2 and n, are the refractive indices of the sample and the IRE respectively. When the incident angle is greater than the critical angle, total internal reflection occurs. As the light is totally reflected at the interface, an exponentially decaying evanescent wave is set up in the rarer outer phase (sample). It is through this evanescent wave that sampling occurs. The exponential decay of the evanescent field into the sample describes the decrease in the electric field perpendicular to the surface, the *Z* direction. Thus the electric field at some distance Z from the nonabsorbing interface is expressed as *(26):*

$$E = E_{,,} \exp\{(-2nA,y\sin^{3}8 - n_{21}^{2})^{\wedge} Z) \quad (2)$$

where E,, is the electric field amplitude at the surface, X, = *X/n,* is the wavelength of the radiation in the denser medium, *X* is the wavelength in free space, 6 is the incident angle, = njAh.and Z is the distance from the surface.

Jt should be mentioned here that the total internal reflection theory is simplified by assuming an infinite plane wave at an interface between semi-infinite nonabsorbing media (26). Even though these assumptions are unrealistic, they make the treatment of internal reflection theory relatively easy and the properties of the evanescent field can be adequately described by Equation 2. The validity of the internal reflection theory developed based *on the* above mentioned assumptions has been demonstrated by several researchers in the past for a variety of applications in the area of interfacial phenomena (9,25,27). Equation 2 can be simplified as:

$$E = E_{,,} \exp(-TIZ) \quad (3)$$

where ***T*** is the exponential constant that is equal to $2nn_1(\sin 3 - n_{,,}^{2})^{1*}$ /

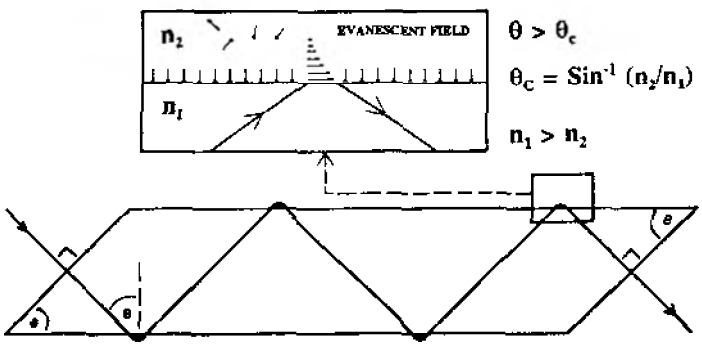

Figure 1. Schematic of light ray undergoing multiple total internal reflections in an IRE.

Depth of Penetration

The depth of penetration of the evanescent field is an important parameter in internal reflection spectroscopy and is particularly significant in the present work. For a nonabsorbing rarer phase, Harrick (9) defined the depth of penetration as the distance from the IRE where the electric field amplitude fails to 1/e of its value at the surface. The depth of penetration, dp, as defined by Harrick is equal to */fr* and is given by:

$$d_{p} = X\ I\ (n,2Tt(siii^{2}e - n_{z}^{2}f) \quad (4)$$

The nomenclature involved with dp is unfortunate since it is often mistaken as the actual depth that is sampled in the IRS experiment. Since the electric field is 37® of its surface value at dp, the depth actually sampled is greater than cy However, the spectral information obtained is most indicative of the spectral characteristics closest to the surface and the contribution of spectral information away from the surface is significantly less according to the exponential decay of the electric field amplitude (Equation 3). It should be mentioned here that the model system (silicon/water) considered in the present study has an outstanding feature, i. e., a large value of $< E_{z}^{2} >$ at the critical angle. This allows for an intense interaction with species at the interface. In other words, the interfacial water species concentrated in the first few layers will experience most of this electric field, hence the resulting spectrum contains important information about interfacial water species.

As mentioned above, the equation for depth of penetration {Equation 4) was derived based on the assumption that the second medium (rarer medium) is a nonabsorbing medium. For relatively low absorbing media such as adsorbed organic surfactants and polymer films, the validity of this equation has been demonstrated by several researchers in the past (9,25,28), However, for highly absorbing rarer medium, such as water, used in this present work. Equation 4 should be modified by taking into account the complex refractive index comprised of the real (n) and imaginary {**K**, attenuation index) parts (29):

$$dp = X / (n,2it(sin^{2}e - n_{21}^{2}(1 + i*)^{2})*) \quad (5)$$

Figure 2 shows the variation in the depth of penetration (calculated using Equation 5) as a function of the incident angle for the silicon/water system being examined in this study. The critical angle for obtaining total internal reflection in this case is approximately 23 degrees as calculated from Equation 1. It can be observed from Figure 2 that the depth of penetration decreases as the incident angle increases.

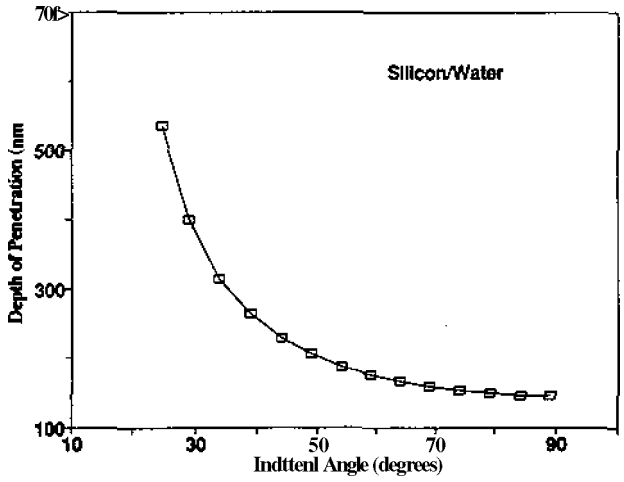

Figure 2. Variation of depth of penetration as a function of incident angle for the silicon/water system.

Depth Profiling by In-SItu FTJR/IRS

As evident from the above, in-situ FTIR/IRS with reactive internal reflection elements should be a powerful analytical technique to study the spectral characteristics of interfacial water. Specifically, it is expected that interfacial water present at various distances from the surface can be described based on the in-situ FTIR/IRS spectral information. In other words, spectral characteristics including band position, intensity, and shape can be examined at different distances from a surface by simply varying the incident angle of the IR beam in the IRE (see Figure 2). The incident angle can, in turn, be varied by changing the face angle of the IRE and the optics of the experiment as will be explained in the experimental section. For the silicon/water system examined in this study, dp values (as calculated from Equation 5) ranging from 153 *nm to about 550 nm* were possible, with the available sampling accessories and optics, for the study of interfacial water by in-situ FTIR/IRS in the MIR region.

Surface Water vs. Balk Water

Internal reflection spectroscopy will allow for the analysis of interfacial water in the region anywhere from a few nanometers to a few hundreds of nanometers near a surface depending upon the optical properties of the solid surfaces and the type of spectroscopy used, i. e., mid-IR (MIR), near-IR (NIR), and Raman. For example, when using Raman internal reflection spectroscopy with a silicon internal reflection element, typically dp values as small as 30 nm can be obtained even though a significant effort is required to enhance *the* extremely weak wafer signals generated with this method. In the MIR, the smallest dp value possible for the silicon/water system examined was 153 nm with the available sampling accessories. It can be noticed from Figure 2 that it becomes very difficult to decrease the dp beyond a certain value at larger incident angles, further away from the critical angle. However, by going to the NIR, these dp values can be further decreased and typically a dp value of about 100 nm can be obtained for the silicon/water system. Of course for the FTIR/IRS study of interfacial water in the NIR region, the IRE must be transparent. Fortunately, most minerals are transparent in the near-IR region which facilitates the study of interfacial water in regions closer to the surface.

It is now clear that the smallest region close to the surface that can be sampled by in-situ FTIR/IRS is in the range of about 150 nm, i. e., about 500 molecular layers from the surface for the silicon/water system in the MIR region. This then raises the question, "Are we really going to be able to

see surface water ?". The answer to *this important* question depends on several *factors* including the extent of interfacial water structuring and the surface sensitivity of the technique used. As discussed in the previous section on depth **of** penetration, the electric field amplitude decays exponentially into the second phase and the majority of the signal comes from the near surface regions even though the total sampling depth is greater than the calculated characteristic depth of penetration. This means that the in-situ FTIR/IRS spectra **of** interfacial water contains information about both surface water and bulk water. As will be discussed in the following section, surface water can be clearly distinguished from the bulk water by the presence of certain band frequencies in the OH stretching region of the water spectra. In fact, in-situ FTIR/IRS will sample both surface and bulk water simultaneously unlike the case for sum frequency generation *(SFG) method where bulk water is* not sampled *at* all (10).

EXPERIMENTAL

Materials

Single crystal silicon and germanium internal reflection elements (50x10x2 mm) used in this study were purchased from Harrick Scientific, NY. Acetone and methanol used in chemical cleaning of the internal reflection elements (IREs) were of reagent grade. Heptane (99%) solvent used in some in-situ FTIR/IRS experiments was purchased from Aldrich and was used as received. The fluorochemical polymer (Fluorad FC-722, *3* M) was used to create a hydrophobic coating at the germanium surface. Millipore (18 Mil) water was used in all the experiments.

Procedures

All the silicon and germanium IREs used in this present study were 50x10x2 mm in dimension. However, the face angles on these IP.Es were different in order to vary the incident angle and achieve the various dp values desired for the study of interfacial water. The IREs were cleaned before each and every experiment to avoid contamination problems. The cleaning of these IREs involved two steps. In the first step, the IREs were thoroughly cleaned and rinsed with acetone/water/methanol/water. Later, the IREs were placed in a Tegai plasma chemical reactor and subjected to argon plasma for 60 minutes *prior* to the FTIR/IRS experiments.

The germanium crystal was coated with a oleophobic-hydrophobic fluorochemical polymer by a spreading technique. The FC-722 polymer is available as a 2% solution in a fluorocarbon solvent (boiling point of 56 °C). This solution was diluted to 0,3-0.5% with an analytical grade solvent, fluorocarbon 113 (1,1,2-trichloro-1,2,2-trifluoroethane; Horiba Instruments Inc.) and then spread over the surface of theciean germanium crystal using a microsyringe. Solvent was evaporated first in the ambient atmosphere at a room temperature of 20-22 °C for 5-10 minutes and next in a clean vacuum oven at temperature of 80-90 °C for 0.5-1 hour. The remaining polymer coating formed a film at the germanium crystal surface with a thickness of 30-50 nm as determined by profiiometry.

Spectra of interfacial water were recorded with a Digilab FTS-40FT-IR spectrometer using a wide-band liquid-nitrogen cooled MCT detector. A twin parallel-mirror reflection 320 internal reflection accessory (Harrick Scientific, NY) was used to hold the stainless steel IRS cell. This liquid IRS cell has a sampling length of 40 mm on both sides of the silicon IRE. IREs with different face angles were used to obtain a desired depth of penetration value for each experiment. The angle on the base plate was also varied in order to obtain different incident angles (always larger than the critical angle for total internal reflection) and consequently different depth of penetration values for these FTIR/IRS experiments. Figure 2 shows a range of typical depth of penetration values that can be obtained at different base plate readings and incident angles with silicon IREs of different face angles.

Interfacial water spectra were generated by taking the absorbance Spectrum after injection into the flow-through IRS cell against the background spectrum of the clean IRE, All spectra were the result of 1024 co-added scans at a resolution of 8 cm^{-1}.

Contact angle measurements (sessile drop method) were done on IREs by using a Rame-Hart contact angle goniometer. These measurements were carried out before and after cleaning the IREs as mentioned above to monitor the surface state and establish its hydrophilic or hydrophobic character prior to each FTIR/IRS interfacial water experiment.

RESULTS AND DISCUSSION

The in-situ FTIR/IRS spectra of inierfacial **wateT** generated at hydrophilic silicon and hydrophobic polymer coated germanium surfaces were studied by examining in detail the OH stretching region between 3000 and 3800 cm^{-1}. This region of the interfacial water spectrum forms a broad band which can **be** deconvoluted into several peaks. The origins and the interpretation of the band frequencies in this region still remain controversial. However, two important regions can be identified in this spectral range without any uncertainty as discussed previously. The spectral features surrounding 3600 cm^{-1} can be assigned *to* the stretching vibration of non-hydrogen bonded or free OH (17,18). On the other hand, the spectral features between 3000 and 3500 cm^{-1} can be ascribed to the stretching vibrations of the hydrogen bonded OH (17,18).

These peaks in the spectral region from 3000 to 3800 cm^{-1} can be used as indicators of the extent of hydrogen bonding present in interfacial water. The extent, or the degree, of hydrogen bonding reflects the extent of structuring of interfacial water. In view of the above, the in-situ FTIR/IRS spectra of interfacial water at silicon surfaces were examined by the analysis of the spectral features in the region from 3000 to 3800 cm^{-1} in order to describe the structure of interfacial water at a hydrophilic silicon surface. Similar spectral features were used by other researchers to characterize interfacial water by Raman IRS (12) and sum frequency generation (18,30) near sapphire and quartz surfaces respectively.

Silicon/Water System

In-situ FTIR/IRS experiments were conducted using three different silicon IREs at various depth of penetration values in order to characterize interfacial water based on spectral information. Extreme care was taken to maintain a similar surface state for each in-situ experiment conducted. Contact angle measurements were conducted to ensure that contaminant free and hydrophilic silicon surfaces had been prepared for each experiment. Contact angles of zero were observed for the argon plasma cleaned silicon crystals indicating a hydrophilic surface. The IREs were transferred to the FTIR sample compartment {dry air purged) immediately after plasma cleaning to avoid any further contamination from the atmosphere.

It should be mentioned thai the surface of silicon single crystals used in this study were found to be very hydrophilic (complete spreading of water) as was evident from the zero contact angles observed after the silicon crystals were cleaned in argon plasma. Also, there was no FTIR spectroscopic evidence for the presence of a hydride layer reported to form due to the dissociation of water at the silicon surface (31),

Figure 3 shows the absorbance spectra of water in the OH stretching region as a function of depth of penetration, dp from the silicon surface. These spectra have been normalized with respect to the number of internal reflections so that the integrated absorbance can be compared (32). Several changes in the spectra with regard to absorbance, peak shape, and position can be noticed from this figure as d_p is increased from 153 nm to 547 nm. It can be noticed from Figure 3 that a distinct change in the shape of the spectra occurred as dp is increased. The peak becomes broader as dp is increased indicating changes in the relative intensities of certain bands as will be clear from the deconvoluted spectra presented in the following paragraphs.

The broad peak in the spectral region shown in Figure 3 was deconvoluted using the Fourier self-deconvolution method available with the Bio-Rad software. This unbiased method provides for useful band narrowing thus enabling the visual identification of broad and overlapping spectral features. These methods have been successfully used by other researchers in the past to study bulk water (12). Figure 4 shows the deconvoluted spectrum of water at a dj, of 153 nm along with the original spectrum. Three peaks centering around 3600, 3400, and 3200 cm^{-1} can be clearly seen from this figure. Other deconvoluted spectra of interfacial water are shown in Figure 5 for three different dp values ranging from 153 nm to 547 nm. The differences in these spectra as dj is varied from 153 nm to 547 nm are immediately obvious and changes in the relative intensities of the three peaks centered about 3600, 3400, and 3200 cm^{-1} can be noticed from this figure. The peak at - 3600 cm^{-1} (free OH stretch) is very weak at d_p= 153 nm and becomes very strong at d_p= 547 nm indicating that the amount of free OH increases as more and more bulk water is sampled at greater depths from the hydrophilic silicon surface. On the other hand, the relative intensities of the peaks - 3400 and ~ 3200 cm^{-1} {hydrogen bonded OH stretch) decrease as the depth of penetration increases from 153 nm to 547 nm. These results suggest that hydrogen bonding is facilitated at the

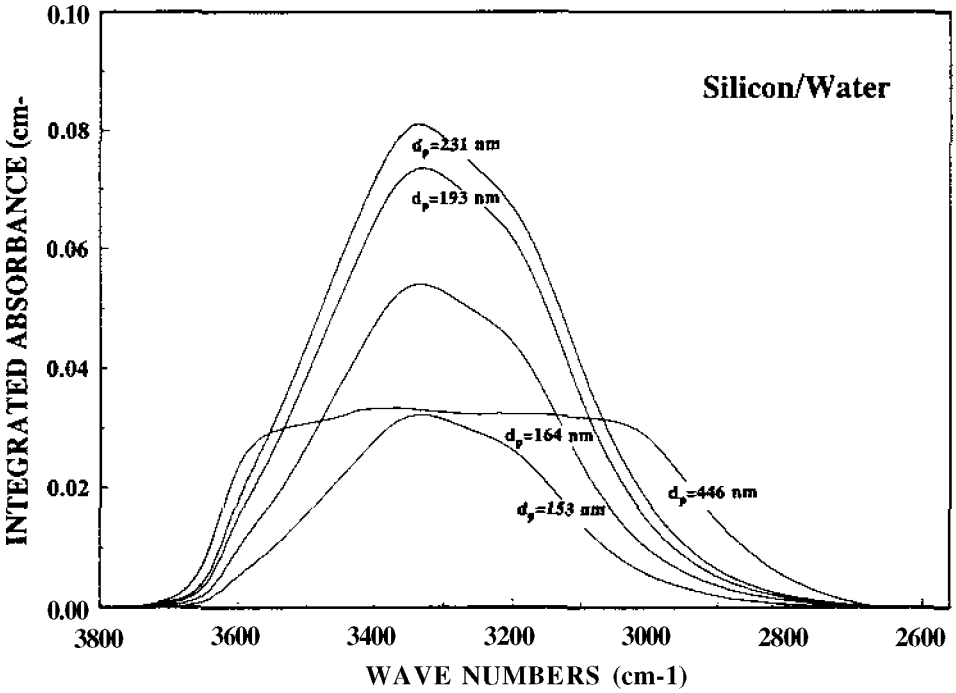

Figure 3. Absorbance spectra of interfacial water as a function of depth of penetration for the silicon/water system in the OH stretching region.

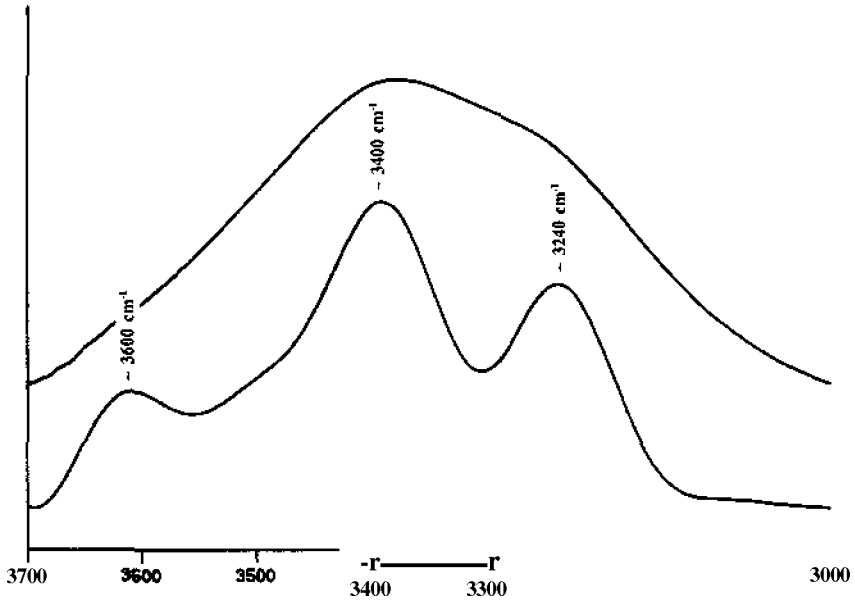

Figure 4. Deconvolved spectrum of water at silicon at a depth of penetration of 153 nm along with the original spectrum in the OH stretching region.

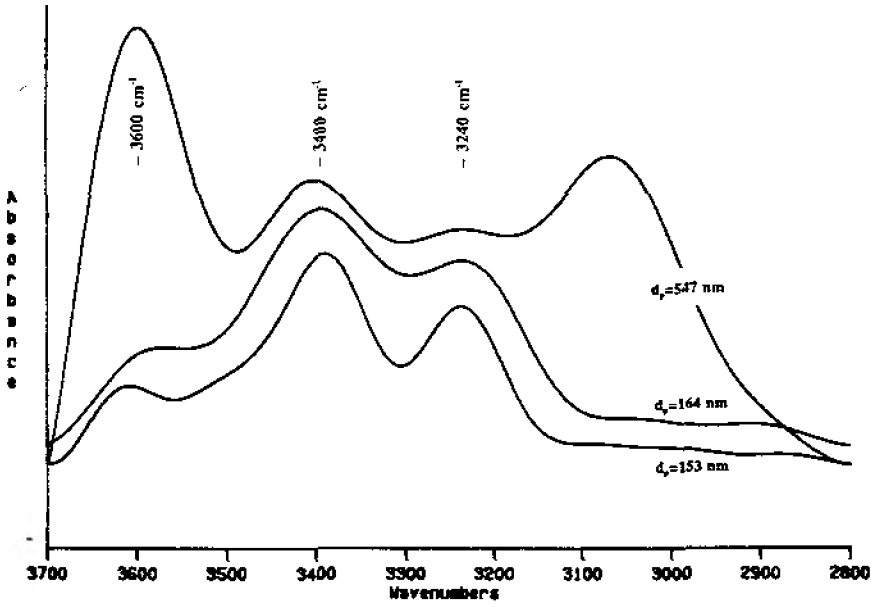

Figure 5. Deconvoluted spectra of interfacial water at various depth of penetration values in the OH stretching region.

hydrophilic silicon surface. A closer look at the deconvoluted spectra for dp values of 153 and 547 nm presented in Figure 6 clearly indicates that water structuring is prevalent near the hydrophilic silicon surface as is evident from the presence of the strong peak at - 3200 cm'. The peak at - 3100 cm' in the deconvoluted spectra shown in Figure 5 seems to be related to the peak at 3600 cm"' since they both decrease in intensity at smaller dp values. This peak has been attributed to the first overtone of the OH bending mode in combination with the Fermi resonance (17,21).

It should be noted that the in-situ FTIR/IRS spectra presented in Figure 3 contain spectral information due 10 the presence of both surface and bulk water as discussed previously. However, it is clearly evident from the spectral features described above that the extent of water structuring (hydrogen bonding/bond ordering) decreases at greater distances from the silicon surface. Furthermore, the relatively high intensity of the peak centered at - 3200 cm"' at the smallest d_p value (1 5 3 nm) is indicative of an ice-like structure in the arrangement of water molecules at the hydrophilic silicon surface. Unfortunately, the depth of penetration could not be decreased below 153 nm for the silicon/water system considered due to limitations discussed previously. Nevertheless, it is very clear from these spectral results that the in-situ FTIR/IRS technique can be used to distinguish between surface and bulk water as is evident from the distinct and obvious changes in the spectra of interfacial water with changes in the depth of penetration. Most importantly, it should be noted that there is a significant change in the shape of the water spectra in the region from 273 to 446 nm where the peak due to free OH (- 3600 cm"') becomes very significant as shown in Figure 3.

Silicon/Heptane System

To further demonstrate that the changes in the spectra of interfacial water at various depths of penetration are due to changes in water structure near the surface, similar studies were conducted at the silicon surface with a non-polar solvent, heptane. Figure 6 shows the absorbance spectra (non-normalized) in the CH stretching region for heptane adsorption at the silicon surface as a function of d_p. It can be noticed from these spectra that there are few changes in the shape and the relative intensities of the

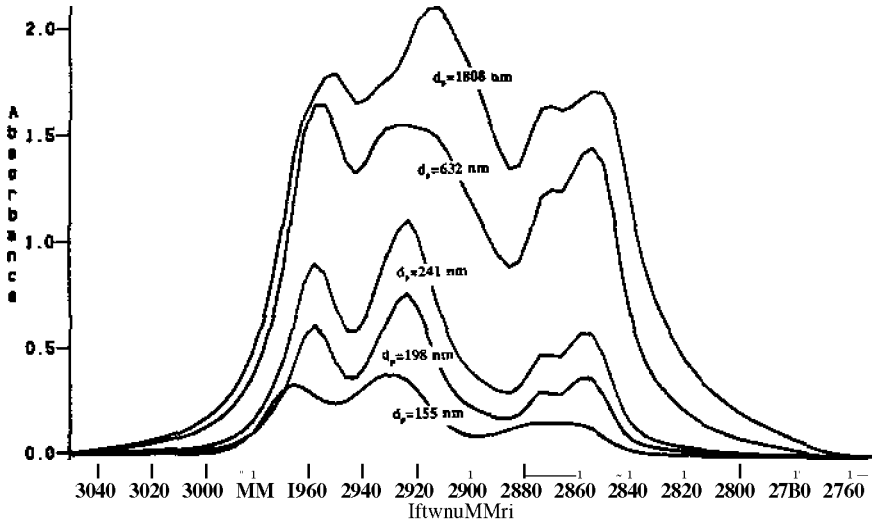

Figure 6. Absorbance spectra of heptane at silicon surface as a function of depth of penetration in the CH stretching region.

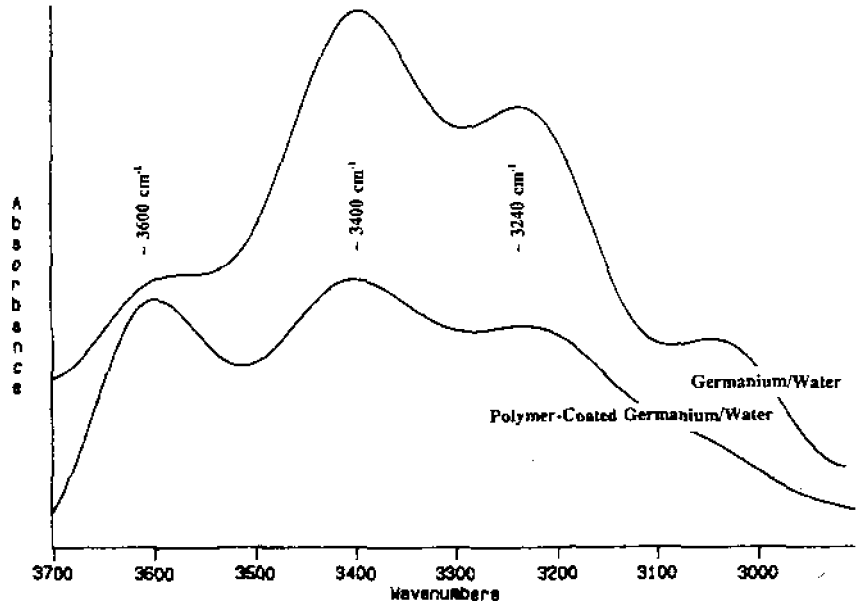

Figure 7. Deconvoluted spectra of interfacial water at germanium and polymer-coated germanium surfaces at a depth of penetration of 128 nm in the OH snetching region.

various bands as **d,** is varied from 155 nm to 1808 nm. By contrast with these results in Figure 6, it **is** evident that the changes in the spectral features of interfacial water at the hydrophilic silicon surface (Figures 3-5) are significant and are not due to bulk spectral distortions (9) but rather are due to changes in the water structure, at different distances from the surface . Such spectral changes ate not observed for nonpolar solvents.

Polymer-Coated Germanium/Water System

In-situ FTIR/IRS experiments were conducted to spectroscopically characterize interfacial water near a hydrophobic surface (polymer-coated germanium single crystal). A germanium single crystal was **used for these** studies simply because of its high refractive index. Also, the fluorochemical **used for** the hydrophobic coating adhered better at the germanium crystal rather than at the silicon surface. Because of the relatively small thickness of the polymer coating (50-80 run). Equation 5 still can be used to calculate depth of penetration values for this system. The hydrophobicity of the polymer-coated germanium IRE was characterized by sessile drop contact angle measurements which yielded a contact angle of 120° **thus** indicating **a** highly hydrophobic surface. Extreme care was taken for the preparation of a uniform hydrophobic film without discontinuities. Examination of these surfaces by optical microscopy indicated that **the** coating was of high quality. For the purpose of comparison, spectra of interfacial water were also generated at the argon plasma cleaned, hydrophilic germanium surface.

Figure 7 shows the deconvolved spectra of interfacial water at the hydrophilic germanium surface and at the hydrophobic polymer-coated germanium surface for a depth of penetration of 128 nm in the OH stretching region. Three bands, centering around 3600, 3400, and 3200 cm^{-1} can be seen in these specna. The relative intensities of these peaks in the water spectrum at the hydrophilic germanium surface indicate the prevalence of more hydrogen bonding similar to the spectral results obtained at the hydrophilic silicon surface at **a** comparable depth of penetration. Water spectrum at the hydrophobic polymer-coated germanium crystal shows a decrease in the relative intensity of the band at - 3200 cm^{-1} (hydrogen bonded OH stretch) whereas the band at - 3600 cm^{-1} (free OH stretch) is much more accentuated when compared to that at the hydrophilic germanium surface as shown in Figure 7. This clearly indicates a decrease in interfacial water structuring near the hydrophobic surface. Similar results were obtained near specially prepared hydrophobic silicon surfaces (32).

SUMMARY **AND** CONCLUSIONS

The spectral results from this work suggests that interfacial water near a hydrophilic surface has more hydrogen bonding and an ordered ice-like structure whereas at a hydrophobic surface there appears to be a decrease **in** the water structuring or hydrogen bonding. These results are in contrast **to** Drost-Hansen's concept **of** a clathrate like water structure near hydrophobic surfaces (33) as well as the recent Raman IRS study of interfacial water by Nickolov et al. (12), However, similar results were reported by **Du** et al. from their SFG experiments for water near hydrophobic and hydrophilic surfaces (30,34). Certainly, additional work needs to be done in order to determine the range of the interfacial water structure at these surfaces. It should be noted that even though the spectra of interfacial water were obtained for significant distances from the surface, because of the high intensity of the electric field amplitude near the surface, it is possible to identify spectral features due to water structure in the regions close to the surface. Efforts are underway to examine the extent of water structuring at different surfaces as well as to increase the surface sensitivity of the FTIR/IRS technique so that water structures closer to the interface can be more clearly detected with minimum interference from bulk water signals. For example, by creating an oxide film at the silicon surface, interfacial water in the first few water layers near the oxide film can be examined with much greater surface sensitivity (35).

In conclusion, it has been demonstrated that the in-situ FTIR/IRS technique can be used to spectroscopically characterize interfacial water at hydrophilic and hydrophobic surfaces. Using this method, the structure of water at different distances from the surface was examined by using appropriate optics and crystal geometries. For the first time, interfacial water has been distinguished from bulk water by analysis of the OH stretching region of the vibrational spectra at different distances from the surface. Preliminary results indicate that a hydrogen bonded ice-like structure prevails at a hydrophilic surface whereas interfacial water structure is diminished near hydrophobic surfaces.

ACKNOWLEDGEMENTS

Financial support from DOE, Office of Basic Energy Sciences, Grant No. DE-FG-03-93ER14315, is gratefully recognized. The authors express their appreciation to Roger Sperline and Jon Kellar for many valuable discussions.

REFERENCES

1. A. W. Adamson, Physical Chemistry of Surfaces, 4th ed., Wiley-Interscience, New York, 1982.
2. J. Leja, Surface Chemistry of Froth Flotation, Plenum Press, New York, 1982.
3. C. Tanford, The Hydrophobic Effect, 2nd ed., John Wiley and Sons, New York, 1980.
4. J. D. Sinclair, "Corrosion of Electronics, the Role of Ionic Substances, J. Electrochemical Soc.. 1988, 135, 89C-95C.
5. J. N. Israeiachvili, Intermolecular and Surface Forces, 2nd ed., Academic Press, New York, 1992.
6. Y. I. Rabinovich and R. H. Yoon, "Use of Atomic Force Microscope for the Measurement of Hydrophobic Forces, Colloids and Surfaces A: Physicochemical and Engineering Aspects, 93, 1994, 263.
7. J. N. Israeiachvili, "Measurements of Hydration Forces Between Macroscopic Surfaces," Chemica Scripta, 25, 1985, 7.
8. Z. Xu, "A Study of Hydophobic Interaction in Fine Particle Coagulation," Ph. D. Dissertation, Virginia Polytechnic Institute and State University, 1990.
9. N. J. Harrick, Internal Reflection Spectroscopy, Harrick Scientific Corporation, New York, 1987.
10. Y. R. Shen, "Surface Properties probed by Second-Harmonic and Sum Frequency Generation," Nature, 337, 1989, 519.
11. R. M. Com and D. A. Higgins, " Optical Second Harmonic Generation as a Probe of Surface Chemistry," Chem. Rev., 94, 1994, 107.
12. Z. S. Nickolov, J. C. Emshaw and J. J. McGarvey, "Water Structure at Interfaces Studied by Total Internal Reflection Raman Spectroscopy," Colloids and Surfaces A:Physicochemical and Engineering Aspects, 76, 1993, 41.
13. D. Eisenberg and W. Kauzamn The Structure and Properties of Water, Oxford University Press, New York, 1969.
14. F. Franks, Ed., Water and Aqueous Solutions, Wiley Interscience, New York, 1972.
15. C. I. Ratcliffe and D. E. Irish, "Vibrational Spectra Studies of Solutions at Elevated Temperatures and Pressures. 5. Raman Studies of Liquid Water upto 300 "C," J. Phy. Chem., 86, 1982, 4897.
16. R. G. Nuzzo, F. A. Fusco and D. L. Allara, "Spontaneously Organized Molecular Assemblies, Preparation and Properties of Solution Adsorbed Monolayers of Organic Disulfides on Gold Surfaces," J. Am. Chem. Soc., 109, 1987, 2358.
17. J. R. Scherer. Advances in Infrared and Raman Spectroscopy, R. J. Clark and R. E. Hester, Eds., Heyden, London, Vol. 5, 1978, 149.
18. Q. Du, R. Superfine, E. Freysz and Y. R. Shen, Phys. Rev. Lett,, 70, 15, 1993, 2313.
19. V. Zhelyaskov, G. Georgiev, Z. Nickolov and N. Miteva, "Behavior of the High Frequency Component of the OH Stretching Raman Band of Water in H202-H20 Mixtures," J. Raman Spectroscopy, 21, 1990, 203.
20. P. A. Giguere, "Bifurcated Hydrogen Bonds in Water," J. Raman Spectroscopy, 15, 5, 1984, 354.
21. J. R. Scherer, M. K. Go and S. Kint, "Raman Spectra and Structure of Water from -10 to 90"," J. Phy. Chem., 77, 1973, 2108.
22. K. Kretzschmar, J. K. Sass and A. M. Bradshaw ," An IR Study of the Adsorption of Water on Ru (001), Surface Science, 115, 1982. 183.
23. H. Ibach and S. Lehwald, "The Bonding of Water Molecules to Plantinum Surface, Surface Science, 91, 1980, 187.
24. G. D' Arrigo, G. Maisano, F. Mallamace, P. Migliardo and F. Wanderlingh, "Raman Scattering and Structure of Normal and Supercooled Water," J. Chem. Phys. , 75, 9, 1981, 4264.

25. J. J. Kellar, W. M. Cross and **J.** D, Miller, " In-Situ Internal Reflection Spectroscopy for the Study of Surfactant Adsorption Reactions using Reactive Internal Reflection Elements," Separation Science and Technology, 25, 1990, 33.
26. F. M. Mirabelia, Internal Reflection Spectroscopy: Review and Supplement. N. J. Harrick, Ed., Harrick Scientific Corporation, New York, 1985, 195.
27. R. P. Sperline, S. Muralidharan and H. Preiser, "In-Situ Determination of Species Adsorbed at a Solid Liquid Interface by Quantitative Infrared Attenuated Total Reflection Spectrophotometry," Langmuir, 3, 1987, 198.
28. **J.** J. Kellar, W. M. Cross and J. D. Miller, "Adsorption Density Calculations from In-situ FT-IR/IRS Data at Dilute Surfactant Concentrations," Applied Spectroscopy, 43, 8, 1989, 1456.
29. G. Mulier, K. Abraham, and M. Schaldach, "Quantitative ATR Spectroscopy: Some Basic Considerations," Applied Optics, 20, 7, 1981, 1182.
30. Q. Da, E. Freysz and Y. R. Shen, "Vibrational Spectra of Water Molecules at Quartz/Water Interfaces," Phys. Rev. Lett., 72, 2, 1994, 238.
31. Y. ***S.*** Chabal, "Hydride Formation on the Si (100): H20 Surface," Phys. Rev. B., 29, 6, 1984, 3677.
32. M. R. Yalamanchili, A. A. Atia and J. D. Miller, "Analysis of Interfacial Water by In-Situ FTIR/Intemal Reflection Spectroscopy," Submitted for Publication, Langmuir, 1995.
33. W. Drost-Hansen, "Structure of Water near Solid Interfaces," Industrial and Engineering Chemistry, 61, 11, 1969, 10.
34. Q. Du, E. Freysz and Y. R. Shen, "Surface Vibrational Spectroscopic Studies of Hydrogen Bonding and Hydrophobicity," Science, 264, 1994, 826.
35. M. R. Yalamanchili and J. D. Miller, unpublished results, 1995.